

## Full Length Article

## Low-frequency plasma activation of nylon 6

Richard Thompson<sup>a</sup>, David Austin<sup>b</sup>, Chun Wang<sup>c</sup>, Anne Neville<sup>c</sup>, Long Lin<sup>a,\*</sup><sup>a</sup> Department of Color Science, School of Chemistry, University of Leeds, Leeds LS2 9JT, UK<sup>b</sup> School of Chemical and Process Engineering, University of Leeds, Leeds LS2 9JT, UK<sup>c</sup> Institute of Functional Surfaces, School of Mechanical Engineering, University of Leeds, Leeds LS2 9JT, UK

## ARTICLE INFO

## Keywords:

Plasma  
 Plasma activation  
 Surface modification  
 Surface functionalization

## ABSTRACT

In the study reported in this paper, a series of reproducible conditions were employed to uniformly functionalize nylon 6 surfaces using a commercially available, low-frequency (40 kHz), low-pressure plasma system, utilizing oxygen plasma as a reactive gas. Initially, the plasma-treated samples were investigated using static contact angle measurements, showing a progressive increase in wettability with increasing plasma activation time between 10 and 40 s. Such an increase in wettability (and therefore increase in adhesive capabilities of the surfaces) was attributed to the creation of surface C-OH, C=O, and COOH groups. These surface-chemical modifications were characterized using x-ray photoelectron spectroscopy (XPS) and static secondary ion mass spectrometry (SSIMS). Surface radical densities were also shown to increase following plasma activation, having been quantified using a radical scavenging method based on the molecule 2,2-diphenyl-1-picrylhydrazyl (DPPH). The samples were imaged and analyzed using scanning electron microscopy (SEM) and atomic force microscopy (AFM), to confirm that there had been no detectable alteration to the surface roughness or morphology. Additionally, the “hydrophobic recovery” or “ageing” of the activated polymer samples, post-plasma treatment, was also investigated in terms of wettability and surface-chemistry, with the wettability of the sample surfaces decreasing over time due to a reduction in surface-oxygen concentration.

## 1. Introduction

The multi-billion dollar surface modification market is constantly increasing in size for polymer materials such as plastics and textiles, due to requirements to impart functional properties into these materials through environmentally benign methods [1]. Plasma technology proves to be an efficient, dry, substrate-independent, and green method for providing these surface treatments, [2,3] avoiding the use of typically inefficient, traditional wet chemical methods [4]. Particularly in the textile industry, there is a significant drive by organizations such as the Zero Discharge of Hazardous Chemicals (ZDHC) towards producing resource efficient processes, completely eradicating the use of harsh chemicals [5]. In addition to being an environmentally friendly process, plasma also has the ability to produce products with a technical advantage, such as anti-microbial surfaces, super hydrophobic surfaces, and flame retardant surfaces [4,6–10].

Worldwide demand for nylon 6 polymers have been increasing in recent years, due to the desirable properties of the material including high tensile strength, wrinkle and abrasion resistance, and high

elasticity [11]. However, unmodified thermoplastics such as nylon 6 cannot meet all modern demands for different applications due to problems such as poor surface wettability, often leading to difficulties when applying functional coatings [12]. Therefore, understanding the fundamental interactions between plasma gases and popular polymer materials such as nylon 6 are crucially important to the development and optimization of plasma treatments for industrial processing [13,14]. The use of different atmospheric and low-pressure plasmas have been reported for the surface treatment of nylon. Some recent examples include the use of atmospheric plasmas to improve the dye absorption and increase the colour strength of dyed nylon fabrics, [15,16] and low-pressure plasmas for the pre-treatment of nylon fabrics prior to coating with carbon nanotubes for fabricating wearable electronic textiles [12]. Low-pressure plasma has also been employed for the etching of nylon fabric meshes for filtration applications [17]. In addition to nylon, there have also been numerous studies of different plasma treatments of other commonly used polymer materials in the textile industry, giving way to range of applications. Examples of such processes and applications include the treatment of polyester fabrics with air, helium, and argon

\* Corresponding author.

E-mail address: [l.lin@leeds.ac.uk](mailto:l.lin@leeds.ac.uk) (L. Lin).<https://doi.org/10.1016/j.apsusc.2021.148929>

Received 9 November 2020; Received in revised form 1 January 2021; Accepted 2 January 2021

Available online 6 January 2021

0169-4332/© 2021 Elsevier B.V. All rights reserved.

plasmas for improvements in the adhesive properties of the fabrics for coating processes, [18,19] and the treatment of cotton with helium and oxygen plasmas to improve the hydrophilicity of fabric, avoiding hazardous chemicals traditionally used in the processing of the material [20,21]. The treatment of silk fabrics with air plasma has also been shown to enhance the performance of the fabrics in pigment-based inkjet printing processes, [22,23] while treating wool with oxygen and nitrogen plasmas has proven to be effective in enhancing the fabric's shrink resistance and anti-pilling properties [24,25].

Plasma is considered to be the fourth aggregation state of matter, and can be identified as a partially ionized gas consisting of a mixture of reactive species including electrons, ions, radicals, neutral atoms, and charged particles [26]. When exposing polymer materials to non-polymerizing, reactive plasma gases such as oxygen, complex plasma-surface interactions on the nano-atomic scale enable material surfaces to be modified, without altering bulk material properties [27]. These modifications can be chemical, physical, or combinations of both, depending on the parameters selected [13]. Cold plasmas are of particular interest for the processing of heat-sensitive polymers (such as plastics and textiles), to prevent thermal decomposition [28]. Low-pressure plasma is a method of producing cold plasma, typically with a radiofrequency (RF) or microwave (MW) discharge. Using this process, materials can be treated with a constant gas flow, usually at pressures ranging from 0.2 to 0.5 mbar [29]. A major advantage of the low-pressure method is the ability to have full parameter control, including the ability to control gas flow in a reproducible manner, and to generate a high concentration of reactive species in a plasma chamber [30]. At the time of writing, few previous studies have reported the use of low-frequency (40 kHz) plasmas for the treatment of polymer materials under low-pressure, with the focus of these studies primarily being placed on the applications of the technology [31–33]. For example, a reported application of the low-frequency oxygen plasma activation of nylon 6 foils is the enhancement of the immobilization of biomolecules on the polymer surface, but the mechanism of the surface activation process is yet to be elucidated [31]. Low-frequency plasmas have a range of advantages when compared to more commonly applied 13.56 MHz (RF) or 2.45 GHz (MW) frequencies, making them a viable alternative. A major advantage is that low-frequencies can generate a higher ion density than the higher RF or MW frequencies, which increases the uniformity of the plasma treatments. Additionally, low-frequency plasma is the most inexpensive form of plasma generation, as it requires the lowest amount of energy to generate [34].

Plasma activation, or “plasma surface functionalization” refers to the increase in surface energy following an attachment or formation of functional groups from interactions with the plasma gas utilized [35]. It was known that typically, in low-pressure plasma systems, this surface modification is accompanied by a physical increase in surface roughness (plasma etching), which involves degradation and mass loss of the surface layers of a material on the nanoscale [36]. This observable mass loss of polymer materials increases as a function of treatment time, [17] and is caused by ion bombardment of the material surface by the reactive plasma species, leading to a physical sputtering process. This process breaks up the surface polymer chains into smaller fragments, with the volatile, low molecular weight species being removed by the vacuum system, hence “etching” the surface [37]. Depending on the plasma system configurations and parameters employed, the etching can either lead to a slight increase in surface roughness, or a more pronounced formation of nano-pores and trenches [38]. For many applications, it is important to avoid this destructive surface roughening during surface modification procedures so that the treated material is not damaged in any way, ensuring that there are no drastic changes to the surface morphology or in the specular component of reflection of the material (change in color) [39]. However, there has been no report on the plasma activation of nylon 6 polymers with low-frequency plasma in which parameters are selected to evade the etching process. Oxygen gas plasmas are often used to activate polymer and textile materials, to

increase the hydrophilicity and adhesive properties of surfaces in preparation for bonding, coating, painting and printing [40]. Oxygen plasma activation proceeds through free radical oxidative reactions that lead to the incorporation of functionalities including carbonyl and hydroxyl groups [41,42]. However, oxygen gas plasmas can also trigger the aforementioned undesired etching effect if the parameters are not carefully selected. At suitably short treatment times with low plasma powers, the triggering of this etching process can be avoided, [13] enabling more energy-efficient conditions to be developed for plasma activation processes.

A major disadvantage of plasma treatments of polymer materials using reactive gases (such as O<sub>2</sub>, N<sub>2</sub> and air) is the deterioration of the treatment level/functionalization level of the materials over time; this is known as the ageing phenomenon, or hydrophobic recovery. This effect can limit the practical applications of the plasma treatments that are used in the hydrophilization of polymers [43]. A number of theories have been postulated in explaining this phenomenon, including the thermodynamically driven reorientation of polar groups away from the surface and into the bulk material, through rotations of the polymer chains. This has the effect of reducing the surface from a high energy state to a lower energy state, and can be considered as a relaxation process [44]. Further explanations for the ageing phenomenon include the migration of low molecular weight, non-polar species from the bulk material to the surface of the polymer, airborne surface contamination, the desorption of low molecular weight oxidised materials into the atmosphere, or contamination due to improper storage conditions [45]. Contact angle measurements prove to be an effective technique in monitoring the hydrophobic recovery of polymers, due to the resulting changes in surface energy caused by the migration and rotations of polymer chains. Following plasma activation, surface contact angle measurements tend to increase with time following this ageing process, due to the decrease in surface energy of the substrate [46].

Although there have been a large number of studies and reviews summarising investigations of different plasma gas treatments on various polymer and textile materials, [6,13,47] the complexity of plasma-substrate interactions has prevented a validated theory that relates and predicts changes in surface properties to specific process variables from being obtained [48]. Despite these complexities, some research groups have designed experimental procedures to systematically understand the mechanisms involved in plasma treatments of polymers, using on-line analytical methods including optical emission spectroscopy, mass spectrometry, and radical imaging methods based on laser-induced fluorescence [49,50]. The variation in plasma systems and plasma generation across the literature means that the parameters required to achieve different plasma effects often have to be determined empirically [51]. Through isolating the surface functionalization/activation plasma process through parameter control, it has been possible to quantify the effects of varying the plasma exposure time of nylon 6 substrates.

In this article, we report on a series of plasma-treatment conditions that were used to activate nylon 6 plastic surfaces using low-frequency (40 kHz) oxygen plasma, without altering the surface morphology or bulk material properties. Analyzing the chemical changes in surface functionalities can often be challenging, as due to a lack of sensitivity, conventional analyses that monitor bulk properties cannot detect the nanoscale changes of functionalities that are induced by plasma treatments [52]. For this reason, a combination of surface-sensitive material characterization and imaging techniques have been utilized, to provide insights into the uniformity and underpinning mechanisms of oxygen plasma surface activation. Additionally, the effect of treatment time on the extent of surface functionalization obtained on the nylon 6 polymer surfaces was explored.

## 2. Experimental section

### 2.1. Materials

Nylon 6 plastic sheets (natural nylon 6, 1.00 mm thickness, 1.14 g cm<sup>-3</sup> density, extruded) were purchased from Direct Plastics Ltd (UK). All solvents (acetone, toluene) used in this study were AR grade  $\geq 99.5\%$  and purchased from Sigma-Aldrich (UK). 2,2-Diphenyl-1-picrylhydrazyl 95% (DPPH) was purchased from Fisher Scientific Ltd (UK). A Branson 1510 ultrasonic cleaning bath (USA) was used for cleaning samples at 160 W prior to plasma treatment. Plasma treatments were performed using a commercially available Diener Zepto Low-Pressure Plasma Laboratory Unit, supplied by Diener electronic GmbH & Co KG (Germany). The system comprised a cylindrical borosilicate glass chamber of 1.7 L volume, two semi-arc electrodes assembled axis-symmetrically on the outer wall of the chamber, two needle valves with mass flow controllers for controlling process gas flow, a pirani gauge for chamber pressure measurement, an analogue timer, and a Pfeiffer Duo 3 rotary-vane vacuum pump (Germany) with an exhaust outlet for the process gas. The system had a working frequency of 40 kHz and had an adjustable power ranging from 0 to 100 W. The low-frequency plasma was generated by a capacitively-coupled plasma (CCP) discharge.

### 2.2. Plasma surface treatment of nylon 6

Nylon 6 plastic sheets of various dimensions were initially cleaned through ultrasonic cleaning with acetone prior to the plasma treatments, to remove any surface impurities, dusts or hydrocarbon contaminants. The samples were fully submerged in a beaker containing acetone that was then placed in an ultrasonic cleaning bath filled with deionised water, operating at a power of 160 W for 10 min. The samples were subsequently left to dry in air. The dry samples were then treated with a low-frequency (40 kHz), low-pressure plasma at a power of 10 W, for exposure times between 10 and 40 s. The samples were placed in the center of the 1.7 L plasma chamber and the oxygen gas flow rate was held constant at 100 cm<sup>3</sup> min<sup>-1</sup> for all treatments, with the working pressure kept between 0.2 and 0.5 mbar. After treatments, the samples were exposed to air for 30 s before being stored under vacuum until analysis.

### 2.3. Surface characterization

Contact angle measurements were performed using a PGX Goniometer. Static contact angles of the nylon 6 plastic sheets were measured by initially placing 4  $\mu$ l sessile water droplets on the polymer surfaces and allowing the droplets to equilibrate for 20 s. The contact angles of the droplets were then measured on the surfaces using a built-in camera. Measurements were performed using three separate samples to test the uniformity and reproducibility of each set of experimental conditions, with two measurements obtained from each of the three samples at different positions. Average values for the contact angles were then obtained from these six measurements, and standard deviations were calculated to show the errors in the measured values. 1  $\times$  1 cm plasma treated nylon 6 samples were analyzed by XPS using a Thermo Fisher K $\alpha$  spectrometer, using monochromatic Al K $\alpha$  radiation (72 W) at pass energies of 150 eV for survey scans, and 40 eV for high resolution scans, with 1.0 eV and 0.1 eV step sizes respectively. The angle between the photoelectron emission direction and plane of the sample was kept constant at 45°, and an area of approximately 400  $\mu$ m was scanned. The XPS utilized low energy electrons and argon ions to prevent charge build-up on the nylon surfaces. Deconvolution of the high resolution C 1s spectra obtained was carried out using the line fitting function on CasaXPS 2.3.19 software, with a Shirley-type background subtraction, and FWHM set to 1.5 eV for all spectral components. For each set of experimental conditions, one spot was analyzed on three separate samples (at a different position on each of the samples) to test the

reproducibility and uniformity of the plasma treatments. Samples (1  $\times$  1 cm) were analyzed by SSIMS using a Hidden Compact SIMS, with a MAXIM-600P detector using a Hidden 6 mm triple quadrupole mass filter with pulse ion detection. The samples underwent Ar<sup>+</sup> primary ion bombardment with a 25nA primary current rastered over a 180  $\times$  180  $\mu$ m area at a 41° angle of incidence from normal, with 5.5 keV impact energy. Surface radical densities were determined through a radical scavenging method, utilizing the molecule DPPH. A calibration graph of DPPH solutions in toluene was initially prepared, enabling the extinction coefficient,  $\epsilon$  to be calculated. 1  $\times$  1 cm untreated and plasma treated nylon 6 samples were immersed in 10 mL solutions of DPPH (1.0  $\times$  10<sup>-4</sup> M) in degassed toluene. The DPPH solution was heated for 3 h at 80 °C. The samples were then cooled to room temperature, and their absorptions were measured with a Varian Cary 50 UV-vis spectrophotometer at 520 nm (the maximum absorbance for DPPH) [53]. Details of the calculations involved in the determination of surface radical densities can be found in the [Supplementary Material](#). Samples were imaged using an FEI Nova 450 SEM. The instrument operated with a field emission gun (FEG) source in standard secondary electron and back-scattered electron modes, operating at 3 kV. All samples were sputter-coated with an ultra-thin iridium layer (2 nm) prior to analysis. AFM images were obtained using a Bruker Innova microscope (USA) with a Nanoscope ADCS controller. A monolithic silicon cantilever with a resonant frequency of 300 kHz and force constant of 40 N/m was utilized in tapping mode, and 1  $\times$  1  $\mu$ m images were obtained. In order to study the ageing properties of the nylon 6 samples following plasma treatment, the samples were exposed to air under ambient conditions for time periods ranging between 0 and 20 days. The samples were then stored under vacuum until being analysed using static contact angle measurements and XPS.

## 3. Results and discussion

### 3.1. The effects of plasma activation on wettability

The wettability of the untreated and plasma treated samples was assessed using static contact angle measurements. From the contact angle measurements displayed in [Fig. 1](#), it can be seen that increasing the treatment times with oxygen plasma led to a relatively linear decrease in contact angle, with the overall hydrophilicity and wettability of the nylon 6 plastic sheets increasing. Although the untreated nylon 6 can already be considered to be slightly hydrophilic (contact angle value of 63.2  $\pm$  1.2°), the longest plasma exposure times saw a significant further increase in hydrophilicity, reaching the lowest value of 38.4  $\pm$  1.4° after 40 s; this exposure time provided the optimum

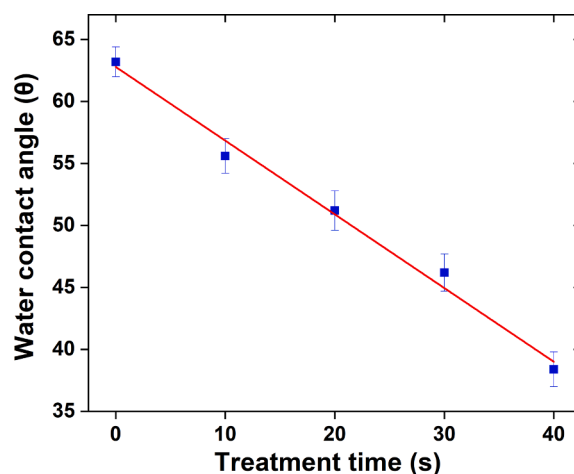


**Fig. 1.** The variation in static water contact angle with plasma treatment time at 10 W.

increase in hydrophilicity without altering the surface morphology. Compared to the untreated nylon 6 samples, there were also gradual reductions in contact angle after 10 s, 20 s, and 30 s respectively. These measurements were rationalized from XPS and SIMS data (discussed later), that confirmed the ability of the oxygen plasma to attach a number of “active” hydrophilic groups within the polymeric structure; this increased the overall wettability of the nylon 6 substrates. The contact angle measurements were not influenced by any changes in surface morphology or roughness, as confirmed by the SEM and AFM images. It is also worth noting that different drop positions were tested on each of the sample surfaces, and the contact angle values did not vary significantly. This suggested that the uniform gas flow that was utilized in the low-pressure plasma treatment method had evenly distributed the surface chemical modifications across all areas of the substrates, with a large degree of reproducibility in the treatments.

### 3.2. The effects of plasma activation on surface chemistry

The elemental composition data in Table 1 confirmed that with increasing plasma activation time, the percentage of carbon present on the nylon 6 surfaces decreased, whilst the oxygen content increased quite significantly. The nitrogen content remained at a similar level, suggesting that the amide linkages within the nylon polymer chains were unaffected by the plasma exposure. There were also residual traces of silicon, calcium, sodium, and magnesium in each of the samples that were attributed to general surface contaminants; they were not reported in this study, due to their negligible amounts (<1%). After treatment for 10 s, the nylon 6 saw an increase in oxygen of 1.7% that suggested the ratio of oxygen-containing functional groups had increased within the polymer chains. The oxygen content then continued to increase progressively up to a maximum of 20.8% (increase of 8.5% compared to the untreated nylon 6) following 40 s of treatment. This was caused through the plasma-generated oxygen radical species reacting with the surface polymer chains of the nylon 6, forming reactive radical sites through hydrogen abstractions of the hydrocarbon backbones. These reactive radical centres then rearranged/recombined or reacted with oxygen upon exposure to air following the treatments, to produce more hydrophilic functionalities such as C-OH, C=O and O-C=O. From the errors shown in Table 1 (representing the standard deviations between the three samples under identical treatment conditions), it can be seen that the general variations for each elemental/functional group peak area were small, with the largest deviation being  $\pm 2.6\%$ . The small variations in the sample data suggested that the extent of the surface modifications induced by the plasma was relatively even at different positions in the plasma chamber, confirming that low-frequency, low-pressure plasma systems have the ability to produce uniform surface modifications to nylon 6 polymers within the plasma chamber.

Deconvolution of the C1s spectra of each of the samples has enabled the increase in surface oxygen content to be characterized further, showing the specific functional groups formed following oxygen plasma treatment. From the high resolution C1s XPS spectra shown in Fig. 2 and the corresponding peak areas presented in Table 1, the changes in surface functionality following plasma activation are shown. These changes are also presented graphically in Fig. 3a. In the untreated nylon 6 spectra displayed in Fig. 2a, the functional groups identified as being present

were C-C, C-N, and C=O. This corresponds to the functionalities present within the nylon 6 repeating unit, with the expected ratios for the nylon structure. Following plasma treatment for 10 s at 10 W, (Fig. 2b) there was a slight increase in the percentage of C=O groups present when compared to the untreated samples (an increase of 1.1%). Also, newly formed C-OH (4.1%) and O-C=O (0.9%) functionalities were identified. They were attributed to the formation of hydroxyl groups and more heavily oxidized species in the form of carboxylic acid chain end groups. These groups were primarily formed through plasma oxidation and bond scission. As the treatment time increased from 10 to 40 s, the atomic % of the newly incorporated C-OH and O-C=O groups also increased to maximum peak areas of 7.2% and 3.3% respectively, while the C-C concentrations decreased substantially.

The trends in Fig. 3a clearly show that the largest increase in peak area with increasing treatment time was seen with the C-OH functional groups, with the O-C=O only seeing a slight increase over time. Having initially increased after 10 s of treatment, the C=O peak areas remained relatively constant between 20 and 40 s, with the C-N groups remaining relatively unchanged following all treatments. This indicated that the amide linkages within the nylon 6 repeat units were unaffected by the plasma activation process, with attachments of hydroxyl groups to the hydrocarbon backbones being the dominant mechanism of action in increasing the surface wettability of the substrates. From the O/C ratios shown in Fig. 3b, a linear increase can be observed for the plasma treated nylon 6 samples with increasing activation time. Due to this increase in surface oxygen content, the increase in O/C ratio directly accounted for the linear decrease in measured contact angle values, and therefore increase in surface energy/hydrophilicity.

To complement the quantitative XPS data, SSIMS analysis was performed (Fig. 4) to provide further details on the chemical species present on the nylon 6 surfaces following oxygen plasma exposure. From the untreated nylon 6 negative ion spectra shown in Fig. 4a, the major peaks observed with the highest normalized intensities appeared at  $m/z = 1^-$  ( $H^-$ ),  $16^-$  ( $O^-$ ),  $26^-$  ( $C_2H^-$ ),  $42^-$  ( $CNO^-$ ),  $83^-$  ( $C_5H_7O^-$ ),  $112^-$  ( $C_6H_{10}NO^-$ ,  $M^-H$ ),  $146^-$  ( $C_7H_{12}NO_2^-$ ), and  $199^-$  ( $C_{12}H_{25}NO^-$ ). The major assigned peaks in the positive ion spectra (Fig. 4b) appeared at  $m/z = 1^+$  ( $H^+$ ),  $16^+$  ( $O^+$ ),  $28^+$  ( $CO^+$ ),  $41^+$  ( $C_2H_3N^+$ ) and  $55^+$  ( $C_3H_3O^+$ ) and  $114$  ( $C_6H_{12}NO^+$ ,  $M^+H^+$ ). All of these peaks can be considered to be expected fragments from the polyamide structure of the nylon 6 repeating unit, correlating to the functionalities present within the polymer. The peaks at  $m/z = 112$  and  $114$  corresponded to the polymer repeating units as  $M^-H$  and  $M^+H^+$  respectively.

The nylon 6 oxygen plasma treated negative ion spectrum for 40 s of plasma exposure at 10 W is displayed in Fig. 4c. The major peaks observed were shown at  $m/z = 1^-$  ( $H^-$ ),  $16^-$  ( $O^-$ ),  $17^-$  ( $OH^-$ ),  $25^-$  ( $C_2H^-$ ),  $26^-$  ( $CN^-$ ),  $36^-$  ( $C_3^-$ ),  $59^-$  ( $C_2H_3O_2^-$ ), and  $112^-$  ( $C_6H_{10}NO^-$ ,  $M^-H$ ). There were also a large number of new peaks with very low intensities that were present in the negative ion spectrum. The assigned peaks in the positive ion spectra (Fig. 4d) appeared at  $m/z = 1^+$  ( $H^+$ ),  $16^+$  ( $O^+$ ),  $17^+$  ( $OH^+$ ),  $28^+$  ( $CO^+$ ),  $36^+$  ( $C_3^+$ ),  $41^+$  ( $C_2H_3N^+$ ),  $55^+$  ( $C_3H_3O^+$ ),  $60^+$  ( $C_2H_4O_2^+$ ), and  $114^+$  ( $C_6H_{12}NO^+$ ,  $M^+H^+$ ). Similarly to the negative ion spectrum, a large number of new fragments with low relative intensities were also observed. Interestingly, in both the negative and positive ion spectra, the intensity of the oxygen peak at  $m/z = 16$  increased following plasma exposure for 40 s. This aids in rationalizing the increase in O/C ratio

**Table 1**

Elemental composition XPS data obtained for untreated and oxygen plasma treated nylon 6 samples.

Elemental composition (%)					C1s peak area (%)				
Treatment time (s)	Carbon	Oxygen	Nitrogen	O/C ratio	C-C	C-N	C=O	C-O(H)	O-C=O
0	76.0 $\pm$ 1.1	12.3 $\pm$ 0.3	10.0 $\pm$ 0.4	0.16 $\pm$ 0.01	69.0 $\pm$ 0.4	16.3 $\pm$ 0.2	14.7 $\pm$ 0.4	0.0 $\pm$ 0.0	0.0 $\pm$ 0.0
10	75.0 $\pm$ 1.3	14.0 $\pm$ 1.0	10.3 $\pm$ 0.4	0.19 $\pm$ 0.02	62.8 $\pm$ 0.9	16.4 $\pm$ 0.2	15.8 $\pm$ 0.6	4.1 $\pm$ 0.3	0.9 $\pm$ 0.2
20	70.5 $\pm$ 1.1	17.7 $\pm$ 0.9	10.1 $\pm$ 0.2	0.25 $\pm$ 0.02	59.9 $\pm$ 2.6	16.2 $\pm$ 0.9	16.4 $\pm$ 1.5	5.9 $\pm$ 0.3	1.6 $\pm$ 0.6
30	69.0 $\pm$ 1.1	18.5 $\pm$ 1.3	10.1 $\pm$ 0.5	0.27 $\pm$ 0.02	59.2 $\pm$ 1.3	15.9 $\pm$ 0.4	15.8 $\pm$ 0.7	7.0 $\pm$ 0.4	2.1 $\pm$ 0.6
40	66.8 $\pm$ 1.4	20.8 $\pm$ 0.7	10.2 $\pm$ 0.7	0.31 $\pm$ 0.02	58.5 $\pm$ 1.9	15.6 $\pm$ 0.3	15.4 $\pm$ 1.6	7.2 $\pm$ 0.7	3.3 $\pm$ 0.3



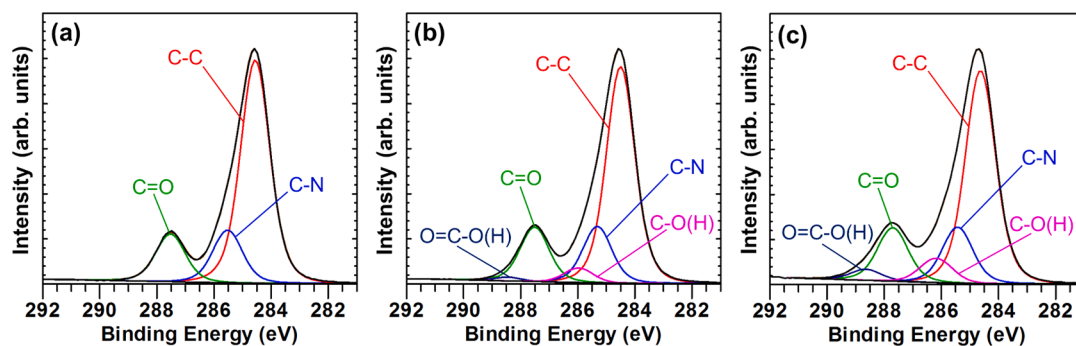


Fig. 2. High resolution C1s XPS spectra with peak fittings of: (a) untreated nylon 6; (b) 10 s, 10 W oxygen plasma treated nylon 6 and (c) 40 s, 10 W oxygen plasma treated nylon 6.

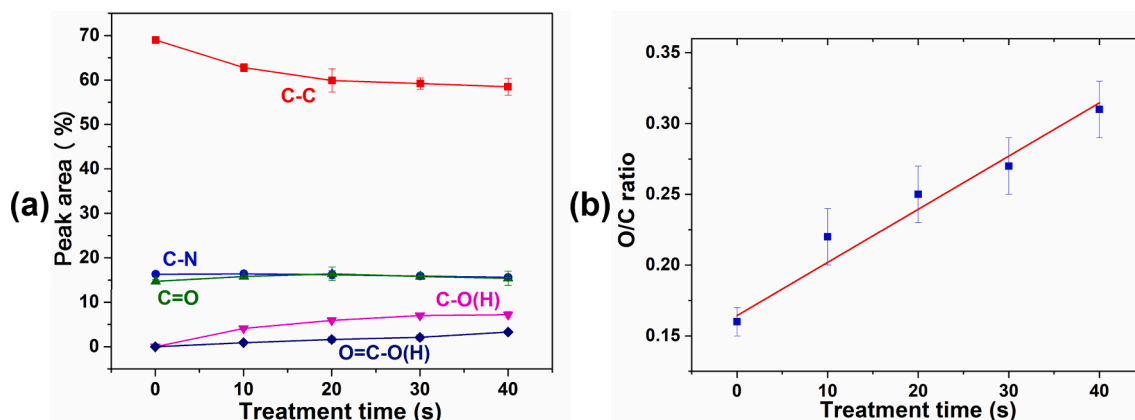


Fig. 3. (a) The observed changes (%) in peak area for the different XPS peak fittings (b) O/C ratios of the plasma treated samples as a function of treatment time.

observed in the XPS spectra, and the increase in wettability. It also confirms that the oxygen plasma incorporated polar oxygen-containing functionalities into the surface structure of the nylon 6 polymer. Additionally, the peak at  $m/z = 17$  that was observed in both the positive and negative ion spectra with high intensities confirmed the presence of hydroxyl groups that had been incorporated into the nylon structures from exposure to the oxygen plasma species. The  $m/z = 112^-$  ( $M^-H^+$ ) and  $114^+$  ( $M^+H^+$ ) peaks in the negative and positive ion spectra respectively were both still present in the plasma treated samples, but their intensities had been vastly reduced. Although peaks with these intensities would not normally be assigned as significant peaks, they provided evidence that a small portion of the original nylon 6 surface structure were still present in the samples following plasma exposure. This suggested that under these low powered and short timescale treatments, the plasma action was not substantial enough to completely eradicate the original surface structure, with a small number of the nylon 6 chains still remaining intact. The peaks at  $m/z = 59^-$  ( $C_2H_3O_2^-$ ), and  $60^+$  ( $C_2H_4O_2^+$ ) were attributed to the formation of carboxylic acid groups in their deprotonated and protonated forms respectively. These polar groups were formed as chain end groups on the polymer chains following plasma induced chain scission and surface oxidation, and confirmed that the formed O-C=O bonds shown in the XPS data can be attributed to carboxylic acid groups. It was evident from both the positive and negative ion spectra of the 40 s plasma treated surfaces that there were no intense peaks with  $m/z$  values  $> 100$ . However, the large number of newly formed, low intensity peaks with  $m/z > 100$  was indicative of chain scission of the polymer chains, disrupting the long-range order in the polymer structures and increasing the extent of fragmentation. The large number of new peaks with low intensity also suggested that the chain scissions induced by the plasma treatments were not selective, and created a large number of new species with different chain lengths.

The surface densities of free radicals, including post-oxidation products such as peroxy radicals formed after exposure of the plasma activated samples to air were quantified using a radical scavenging method, which utilized the molecule DPPH. The extinction coefficient for DPPH in toluene was measured to be  $11,057 \text{ L mol}^{-1} \text{ cm}^{-1}$ , which is similar to values previously reported in the literature [54]. From the calculated values of free radical surface density shown in Fig. 5, there was a general trend of increasing radical density with increasing plasma treatment time. There were some initial surface radicals detected in the untreated nylon 6 samples, which could be attributed to the DPPH undergoing undesired side reactions with the aliphatic chains in the nylon structure. Between the 10 s and 40 s plasma treated samples, the radical surface densities were all in the range of  $7.0\text{--}11.0 \times 10^{-9} \text{ mol cm}^{-2}$ , with a general increase in radical density with increasing treatment time. These values were of a similar order to that of previously reported radical densities for plasma treated polymer materials [53,55]. The presence of radicals on the surface confirmed that plasma activation led to the formation of reactive radical sites, through hydrogen abstractions of the nylon 6 hydrocarbon backbone from oxygen radical species in the plasma. This aided in explaining the incorporation of oxygen containing hydroxyl and carbonyl groups, due to reactions of oxygen plasma species with these radical sites. In addition, the presence of surface radicals also accounted for the structural rearrangements that occurred following chain scission, forming carboxylic acid chain end groups (detected in XPS and SSIMS analysis). The error bars were particularly large for each of the treated samples, which can be attributed to a variety of potential interfering factors in the DPPH radical scavenging method, such as the swelling effects of the toluene solvent on the nylon polymer surface, some of the radicals being quenched upon exposure to air following plasma treatment, and potential side reactions that can occur between the highly reactive DPPH and some of the aliphatic chains within the

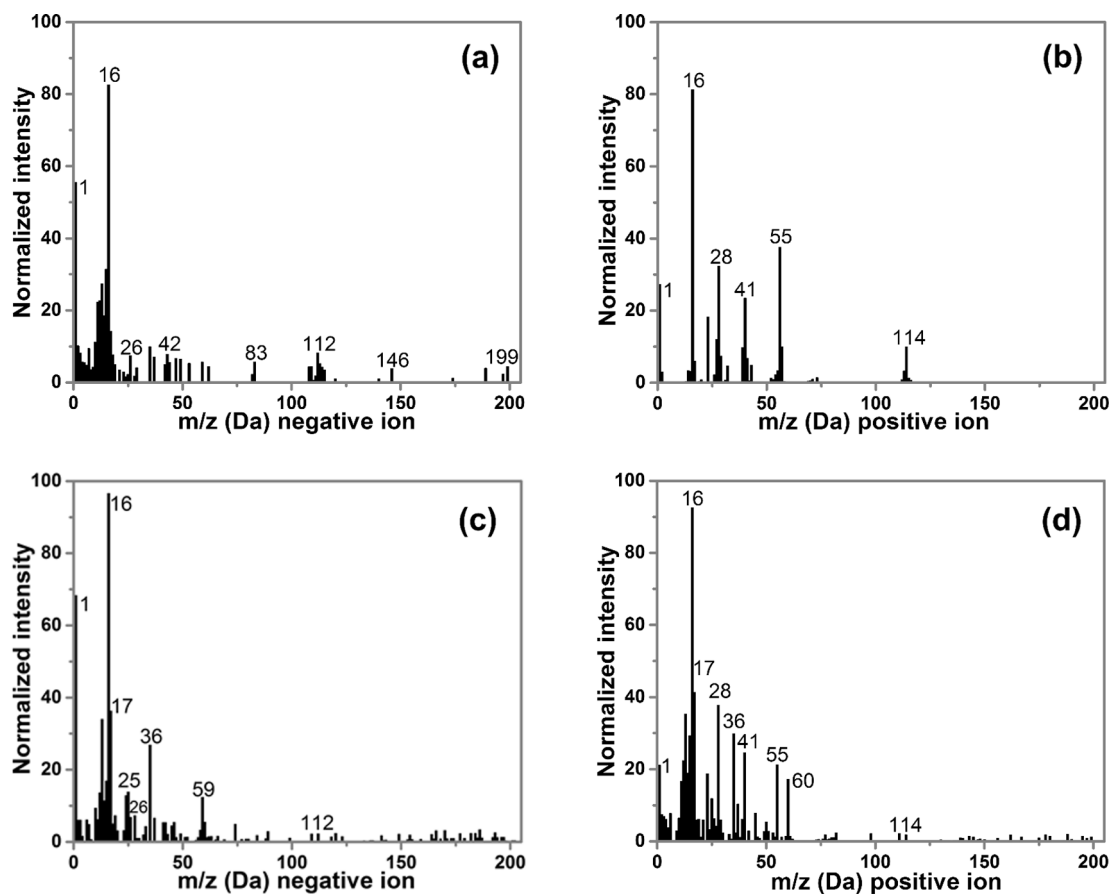


Fig. 4. (a) SSIMS negative ion spectrum and (b) positive ion spectrum for untreated nylon 6. (c) SSIMS negative ion spectrum and (d) positive ion spectrum for oxygen plasma treated nylon 6 for 40 s at 10 W.

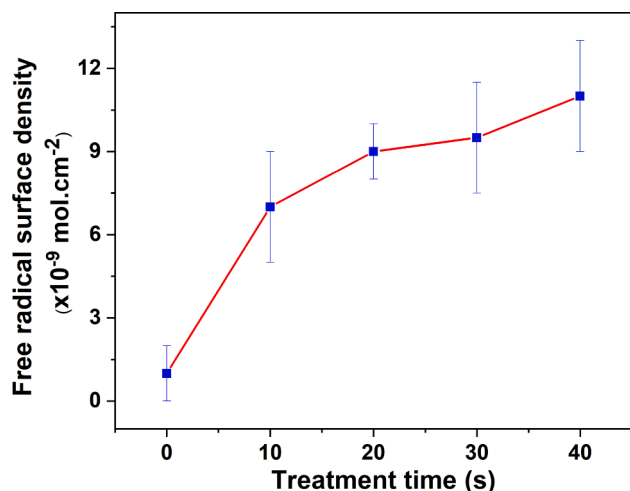


Fig. 5. The free radical surface densities of untreated and oxygen plasma treated nylon 6 samples between 10 and 40 s at 10 W.

polymer structure. Although this method of detecting and quantifying surface radicals has several limitations, such as the radical scavenger DPPH not having the ability to distinguish between specific radical species, and the aforementioned interfering chemical species, it is still useful in providing mechanistic insights into the complex surface modification induced by plasma activation. The method is effective in complementing the XPS and SIMS data, providing information about the scale of the radical surface density following plasma activation, and

showing the general trend of increasing radical density with increasing treatment time.

### 3.3. Surface morphology and roughness

The SEM images in Fig. 6 show the surface morphology of the nylon 6 sheets both before and after low power (10 W) oxygen plasma exposure. The images confirm that there were no significant physical changes to the polymer surface morphology following exposure (40 s) to the plasma at 10 W. Fig. 6a shows that the untreated nylon 6 sheets were generally smooth with occasional grooves and a number of embedded surface particles. The EDX spectra of these particles were analyzed and shown to have near-identical spectra to the smooth areas of the surface (see Supplementary Material). They were attributed to surface agglomerates formed from the manufacturing and processing of the nylon sheets. After oxygen plasma treatment for 40 s (Fig. 6b), the surface of the polymer sheets and embedded particles did not change. Following longer treatment times, there were obvious changes to the surface morphology, with a significant increase in surface roughness due to plasma etching (see Supplementary Material for examples). This confirmed that under the selected conditions in this study, the conditions were non-destructive to the outer surface layers of the substrate, and the increase in hydrophilicity shown in the contact angle measurements (Fig. 1) was caused entirely by a chemical change.

AFM was used to provide further details regarding the quantification of surface roughness of the samples before and after plasma activation. It is a well-known phenomenon that low-pressure plasma treatments of polymer materials generally have the effect of increasing the surface roughness [38]. However, under the conditions proposed in this study, the SEM images showed no obvious changes in surface morphology. The

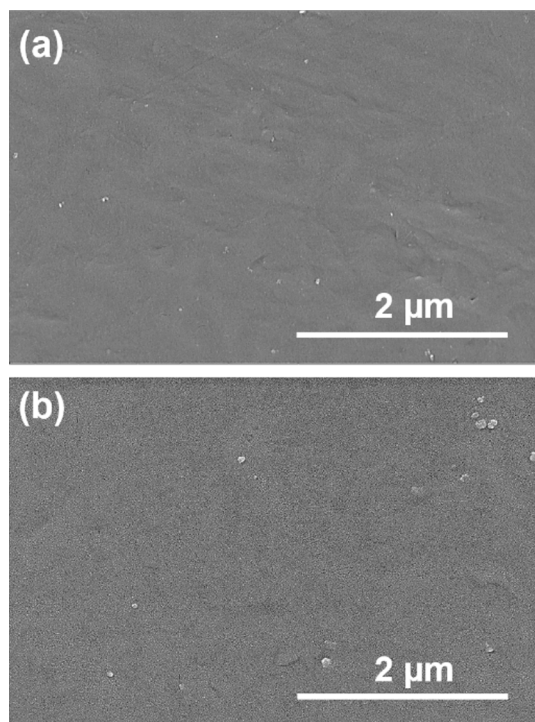


Fig. 6. SEM images of (a) untreated nylon 6 and (b) oxygen plasma treated nylon 6 for 40 s at 10 W.

AFM images and corresponding surface roughness measurements shown in Fig. 7 were in agreement with the SEM images, and confirmed that there had been no induced surface roughness in the plasma activated samples. The root mean square roughness (Rq) values for the untreated (7.47 nm) and 40 s oxygen plasma treated (6.96 nm) were both very similar, showing that the plasma had not increased the surface

roughness. Although the roughness Rq value was slightly lower for the plasma treated surface, this difference was attributed to the general variation between different areas of the manufactured sheets that were present in all samples. The roughness average (Ra) values for the untreated (6.07 nm) and 40 s plasma treated (5.64 nm) were also both very similar, further confirming the lack of morphological change induced by the plasma. Both samples showed generally smooth surfaces, with small areas of mild roughness. The highest points on the AFM images were attributed to the embedded surface particles, which had heights varying between 40 and 50 nm. The AFM data further confirmed that the plasma activation process that occurred under the selected conditions was an entirely surface chemical driven process, with no observed physical change in the nano-surface roughness or appearance.

### 3.4. Ageing of samples post-plasma treatment

The graph in Fig. 8a shows the observed decrease in surface wettability in the oxygen plasma activated nylon 6 samples, with subsequent ageing in air for 20 days. The samples initially saw a sharp increase in hydrophobic recovery, particularly following 1–5 days of ageing. This increase in hydrophobicity then started to become more gradual and levelled off after approximately 14 days, with prolonged exposure to air. The samples that had undergone shorter treatment times (10–20 s) showed a slower initial hydrophobic recovery than the longer treatments (30–40 s), but the final contact values obtained were much higher for the shorter treatment times, indicating a higher degree of hydrophobicity. However, the samples treated for 40 s, had an overall increase in contact angle of  $19.8^\circ$  over the 20 day period, while the samples treated for 10 s only increased by  $6.5^\circ$ , indicating that larger degrees of plasma-surface functionalization resulted in larger increases in the extent of hydrophobic recovery. This hydrophobic recovery was attributed to the reorientation of attached polar surface functionalities through the diffusion of oxidised low molecular weight species into the bulk material, and rotations of polar moieties away from the surface. This is a thermodynamically driven process that shifted the surface

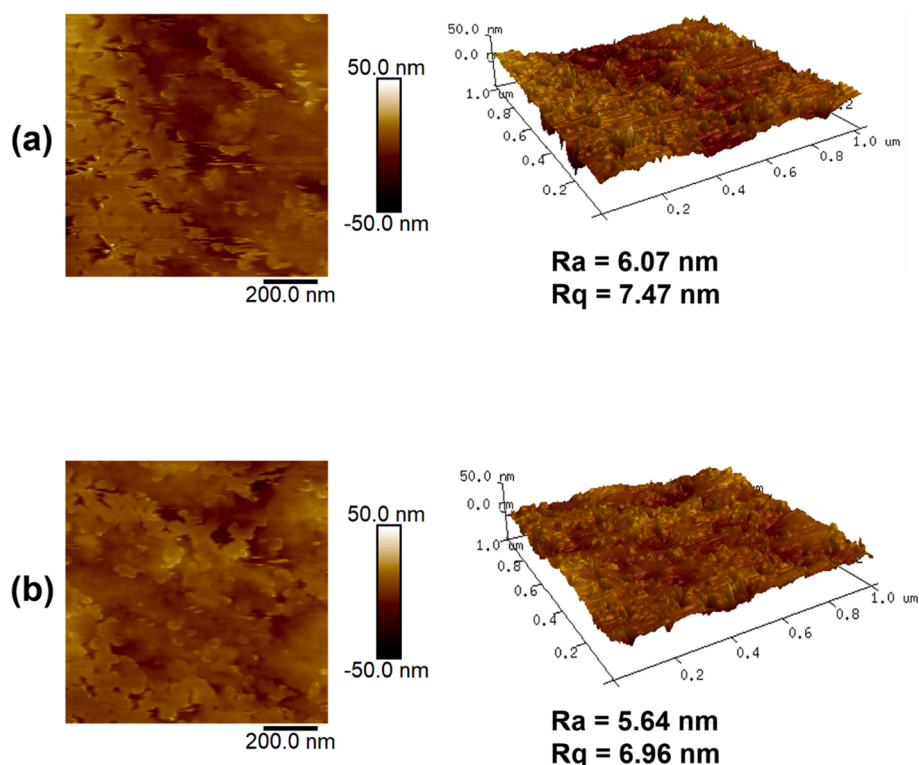


Fig. 7. AFM images of: (a) untreated nylon 6; (b) oxygen plasma treated nylon 6 for 40 s at 10 W.

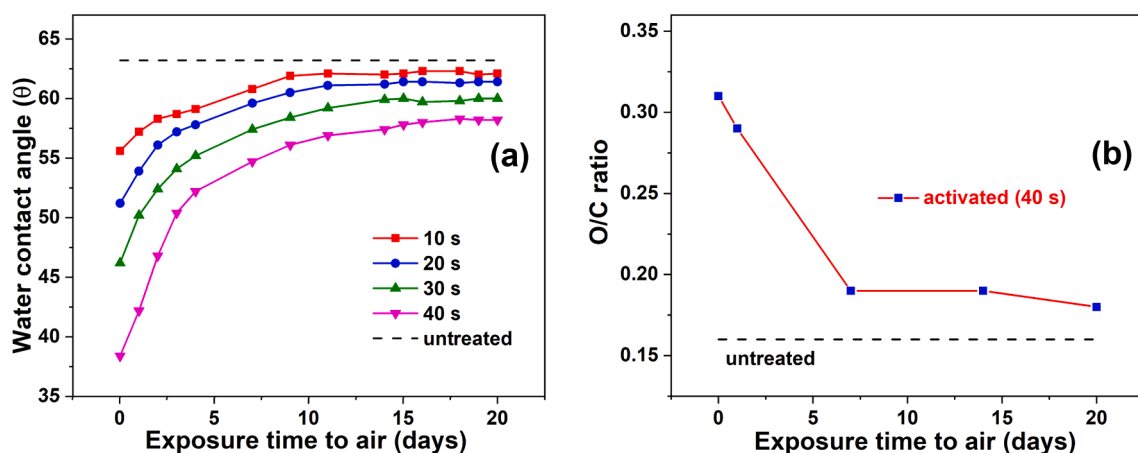


Fig. 8. Graphs showing (a) static contact angle measurements and (b) O/C ratios (determined through XPS) of nylon 6 samples with increasing exposure time to air following plasma activation.

energy from a high energy (polar) state to a lower energy, and more stable state [27]. It was clear that none of the plasma activated nylon samples had fully reverted back to their initial surface wettability, suggesting that some of the attached polar functionalities present on the modified surfaces had remained. This is likely to have been due to some of the attached polar groups having intermolecular interactions with the water molecules in the air, which kept the groups at the surface.

XPS analysis was used to rationalize the trends in hydrophobic recovery seen in the contact angle measurements. Fig. 8b shows O/C ratios for the aged nylon 6 samples that were initially treated with plasma for 40 s at 10 W. The initial reduction in O/C ratio was slight after 1 day of ageing, from 0.31 to 0.29. This decrease was much greater after 7 days to 0.19, at which point the O/C ratio levelled off, which appeared to follow the trend of increasing hydrophobic recovery seen through the contact angle measurements. It was clear that the polar groups had been released from the surface, through the thermodynamically favourable reorientation of the high energy polar groups away from the surface. The oxygen content did not drop to its initial untreated atomic % following 20 days of ageing for the activated sample, which can be attributed to the small amount of moisture present in air, which could have interacted with some of the polar groups through hydrogen bonding, preventing them from reorienting away from the surface, hence keeping interfacial energy higher than the unmodified surface.

#### 4. Conclusions

Through studying the effects of low-frequency, low-pressure oxygen plasma treatments on nylon 6 plastic sheets, mechanistic understandings of plasma activation in terms of physical properties, surface-chemistry, and morphology/roughness have been formed which can then be applied for use in the material processing and manufacturing industries for both plastics and textiles. The ageing of the activated samples following exposure to air has also been investigated. It has been found that activation increased the hydrophilicity of the nylon 6 surfaces, with increasing treatment time also enhancing this increase. XPS, SSIMS, and radical scavenging methods were used to rationalize this increase in wettability in terms of surface chemistry, revealing, for the first time, that due to the combination of: 1) oxygen plasma increasing the number of attached polar functional groups (C-OH, C=O, COOH); 2) the plasma increasing the fragmentation of nylon 6 polymer chains through oxidation and chain scission; 3) the plasma increasing the surface radical density with increasing treatment time, the hydrophilicity of the substrates increased. SEM and AFM imaging were then used to confirm that under the selected conditions for this study, there were no changes to the surface morphology or roughness, unlike many previously reported studies on low-pressure plasma treatments. Potential applications for

the process include being used as prerequisite for applying coatings/paints to enhance coating adhesion, or as a general method for increasing the wettability of materials for bonding or printing, without inducing surface degradation or alterations in morphology.

#### Credit author statement

The project was jointly conceptualised by Long Lin and Richard Thompson.

Long Lin supervised the research project.

Richard Thompson carried out all experimental work.

David Austin assisted with the AFM analyses and interpretations.

Chun Wang and Anne Neville assisted with the SIMS analyses and interpretations.

#### Declaration of Competing Interest

The authors declare that they have no known competing financial interests or personal relationships that could have appeared to influence the work reported in this paper.

#### Acknowledgment

The authors would like to thank the University of Leeds for providing the funding. XPS data collection was performed at the EPSRC National Facility for XPS ("HarwellXPS"), operated by Cardiff University and UCL.

#### Appendix A. Supplementary data

Supplementary data to this article can be found online at <https://doi.org/10.1016/j.apsusc.2021.148929>.

#### References

- [1] U. Cvelbar, J.L. Walsh, M. Černák, H.W. de Vries, S. Reuter, T. Belmonte, C. Corbella, C. Miron, N. Hojnik, A. Jurov, H. Puliyalil, M. Gorjanc, S. Portal, R. Laurita, V. Colombo, J. Schäfer, A. Nikiforov, M. Modic, O. Kylian, M. Polak, C. Labay, J.M. Canal, C. Canal, M. Gherardi, K. Bazaka, P. Sonar, K.K. Ostrikov, D. Cameron, S. Thomas, K.-D. Weltmann, White paper on the future of plasma science and technology in plastics and textiles, *Plasma Processes and Polymers* 16 (2019) 1700228.
- [2] L. Yu, G.Y. Chen, H. Xu, X. Liu, Substrate-Independent, Transparent Oil-Repellent Coatings with Self-Healing and Persistent Easy-Sliding Oil Repellency, *ACS Nano* 10 (2016) 1076–1085.
- [3] R.M. Aileni, L. Chiriac, S. Albici, A. Subtirica, L.-C. Dinca, Aspects of the hydrophobic effect sustainability obtained in plasma for cotton fabrics, *Industria textilă* 070 (2019) 205–210.
- [4] C. Ma, L. Wang, A. Nikiforov, Y. Onyshchenko, P. Cools, K. Ostrikov, N. De Geyter, R. Morent, Atmospheric-pressure plasma assisted engineering of polymer surfaces: From high hydrophobicity to superhydrophilicity, *Applied Surface Science* 535 (2021), 147032.



- [5] N.W.M. Edward, P. Goswami, Plasma-based treatments of textiles for water repellency, in: J. Williams (Ed.), *Waterproof and Water Repellent Textiles and Clothing*, Woodhead Publishing, 2018, pp. 215–232.
- [6] A. Zille, F.R. Oliveira, A.P. Souto, Plasma Treatment in Textile Industry, *Plasma Processes and Polymers* 12 (2015) 98–131.
- [7] N.K. Vu, A. Zille, F.R. Oliveira, N. Carneiro, A.P. Souto, Effect of Particle Size on Silver Nanoparticle Deposition onto Dielectric Barrier Discharge (DBD) Plasma Functionalized Polyamide Fabric, *Plasma Processes and Polymers* 10 (2013) 285–296.
- [8] M. Jimenez, N. Lesaffre, S. Bellayer, R. Dupretz, M. Vandenbossche, S. Duquesne, S. Bourbigot, Novel flame retardant flexible polyurethane foam: plasma induced graft-polymerization of phosphonates, *RSC Advances* 5 (2015) 63853–63865.
- [9] P. Nguyen-Tri, F. Altıparmak, N. Nguyen, L. Tuduri, C.M. Ouellet-Plamondon, R. E. Prud'homme, Robust Superhydrophobic Cotton Fibers Prepared by Simple Dip-Coating Approach Using Chemical and Plasma-Etching Pretreatments, *ACS, Omega* 4 (2019) 7829–7837.
- [10] M. Zhang, J. Pang, W. Bao, W. Zhang, H. Gao, C. Wang, J. Shi, J. Li, Antimicrobial cotton textiles with robust superhydrophobicity via plasma for oily water separation, *Applied Surface Science* 419 (2017) 16–23.
- [11] C. Wang, F. Hu, K. Yang, T. Hu, W. Wang, R. Deng, Q. Jiang, H. Zhang, Preparation and properties of nylon 6/sulfonated graphene composites by an in situ polymerization process, *RSC Advances* 6 (2016) 45014–45022.
- [12] W. Zhang, L. Johnson, S.R.P. Silva, M.K. Lei, The effect of plasma modification on the sheet resistance of nylon fabrics coated with carbon nanotubes, *Applied Surface Science* 258 (2012) 8209–8213.
- [13] R.A. Jelil, A review of low-temperature plasma treatment of textile materials, *Journal of Materials Science* 50 (2015) 5913–5943.
- [14] A. Albéndiz García, E. Rodríguez-Castellón, D. Peláez Millas, Surface modification of thermoplastics by low-pressure microwave O<sub>2</sub> plasma treatment for enhancement of the adhesion of the interface box/encapsulating resin and the influence on film capacitors operating under extreme humidity conditions, *Applied Surface Science* 513 (2020), 145764.
- [15] A. Haji, A. Mousavi Shoushtari, M. Mirafshar, Natural dyeing and antibacterial activity of atmospheric-plasma-treated nylon 6 fabric, *Coloration Technology* 130 (2014) 37–42.
- [16] F.R. Oliveira, A. Zille, A.P. Souto, Dyeing mechanism and optimization of polyamide 6,6 functionalized with double barrier discharge (DBD) plasma in air, *Applied Surface Science* 293 (2014) 177–186.
- [17] H.S. Salapare, T. Darmanin, F. Guittard, Reactive-ion etching of nylon fabric meshes using oxygen plasma for creating surface nanostructures, *Applied Surface Science* 356 (2015) 408–415.
- [18] B. Kutlu, B. Sari, Adhesion improvement at polyester fabric-silicone rubber interface by plasmas of argon and air to obtain conveyor belt, *Industria Textilă* 70 (2019) 470.
- [19] C. Zhang, M. Zhao, L. Wang, L. Qu, Y. Men, Surface modification of polyester fabrics by atmospheric-pressure air/He plasma for color strength and adhesion enhancement, *Applied Surface Science* 400 (2017) 304–311.
- [20] L. Tian, H. Nie, N.P. Chatterton, C.J. Branford-White, Y. Qiu, L. Zhu, Helium/oxygen atmospheric pressure plasma jet treatment for hydrophilicity improvement of grey cotton knitted fabric, *Applied Surface Science* 257 (2011) 7113–7118.
- [21] P. Pransilp, M. Pruettiphap, W. Bhanthumnavin, B. Paosawatyanong, S. Kiatkamjornwong, Surface modification of cotton fabrics by gas plasmas for color strength and adhesion by inkjet printing, *Applied Surface Science* 364 (2016) 208–220.
- [22] C. Zhang, L. Wang, M. Yu, L. Qu, Y. Men, X. Zhang, Surface processing and ageing behavior of silk fabrics treated with atmospheric-pressure plasma for pigment-based ink-jet printing, *Applied Surface Science* 434 (2018) 198–203.
- [23] C. Zhang, F. Guo, H. Li, Y. Wang, Z. Zhang, Study on the physical-morphological and chemical properties of silk fabric surface modified with multiple ambient gas plasma for inkjet printing, *Applied Surface Science* 490 (2019) 157–164.
- [24] S. Zanini, A. Citterio, G. Leonardi, C. Riccardi, Characterization of atmospheric pressure plasma treated wool/cashmere textiles: Treatment in nitrogen, *Applied Surface Science* 427 (2018) 90–96.
- [25] C.W. Kan, K. Chan, C.W.M. Yuen, M.H. Miao, Low Temperature Plasma on Wool Substrates: The Effect of the Nature of the Gas, *Textile Research Journal* 69 (1999) 407–416.
- [26] T. Felix, J.S. Trigueiro, N. Bundaleski, O.M.N.D. Teodoro, S. Sérgio, N.A. Debacher, Functionalization of polymer surfaces by medium frequency non-thermal plasma, *Applied Surface Science* 428 (2018) 730–738.
- [27] E. Kraus, L. Orf, B. Baudrit, P. Heidemeyer, M. Bastian, R. Bonenberger, I. Starostina, O. Stoyanov, Analysis of the low-pressure plasma pretreated polymer surface in terms of acid–base approach, *Applied Surface Science* 371 (2016) 365–375.
- [28] D. Štular, G. Primc, M. Mozetič, I. Jerman, M. Mihelčič, F. Ruiz-Zepeda, B. Tomšič, B. Simončič, M. Gorjanc, Influence of non-thermal plasma treatment on the adsorption of a stimuli-responsive nanogel onto polyethylene terephthalate fabric, *Progress in Organic Coatings* 120 (2018) 198–207.
- [29] M.Y. Naz, S. Shukrullah, Y. Khan, A. Ghaffar, N.U. Rehman, S.J.H.E.C. Ullah, Actinometry study on dissociation fraction in low pressure capacitively coupled Ar–O<sub>2</sub> mixture plasma, *High Energy Chemistry* 49 (2015) 449–458.
- [30] L. Bárdos, H. Baránková, Plasma processes at atmospheric and low pressures, *Vacuum* 83 (2008) 522–527.
- [31] F. Wieland, R. Bruch, M. Bergmann, S. Partel, G.A. Urban, C. Dincer, Enhanced Protein Immobilization on Polymers - A Plasma Surface Activation Study, *Polymers* 12 (2020) 104.
- [32] M. Siciński, D.M. Bieliński, H. Szymanowski, T. Gozdek, A. Piątkowska, Low-temperature plasma modification of carbon nanofillers for improved performance of advanced rubber composites, *Polymer Bulletin* 77 (2020) 1015–1048.
- [33] A. Cireli, B. Kutlu, M. Mutlu, Surface modification of polyester and polyamide fabrics by low frequency plasma polymerization of acrylic acid, *Journal of Applied Polymer Science* 104 (2007) 2318–2322.
- [34] Y. Chen, D. Shi, Y. Chen, X. Chen, J. Gao, N. Zhao, C.-P. Wong, A. Facile, Low-Cost Plasma Etching Method for Achieving Size Controlled Non-Close-Packed Monolayer Arrays of Polystyrene Nano-Spheres, *Nanomaterials* 9 (2019) 605.
- [35] S. Kaya, P. Rajan, H. Dasari, D.C. Ingram, W. Jadwisieniczak, F. Rahman, A Systematic Study of Plasma Activation of Silicon Surfaces for Self Assembly, *ACS Applied Materials & Interfaces* 7 (2015) 25024–25031.
- [36] P. Zhao, N. Qin, C.L. Ren, J.Z. Wen, Surface modification of polyamide meshes and nonwoven fabrics by plasma etching and a PDA/cellulose coating for oil/water separation, *Applied Surface Science* 481 (2019) 883–891.
- [37] R. Morent, N. De Geyter, J. Verschuren, K. De Clerck, P. Kiekens, C. Leys, Non-thermal plasma treatment of textiles, *Surface and Coatings Technology* 202 (2008) 3427–3449.
- [38] I. Junkar, U. Cvelbar, A. Vesel, N. Hauptman, M. Mozetič, The Role of Crystallinity on Polymer Interaction with Oxygen Plasma, *Plasma Processes and Polymers* 6 (2009) 667–675.
- [39] H.-R. Lee, D.-J. Kim, K.-H. Lee, Anti-reflective coating for the deep coloring of PET fabrics using an atmospheric pressure plasma technique, *Surface and Coatings Technology* 142–144 (2001) 468–473.
- [40] A. Vesel, M. Mozetic, New developments in surface functionalization of polymers using controlled plasma treatments, *Journal of Physics D: Applied Physics* 50 (2017), 293001.
- [41] K. Tsougeni, N. Vourdas, A. Tserepi, E. Gogolides, C. Cardinaud, Mechanisms of Oxygen Plasma Nanotexturing of Organic Polymer Surfaces: From Stable Super Hydrophilic to Super Hydrophobic Surfaces, *Langmuir* 25 (2009) 11748–11759.
- [42] X. Yuan, L. Ma, J. Zhang, Y. Zheng, Simple pre-treatment by low-level oxygen plasma activates screen-printed carbon electrode: potential for mass production, *Applied Surface Science* 148760 (2020).
- [43] M. Mortazavi, M. Nosonovsky, A model for diffusion-driven hydrophobic recovery in plasma treated polymers, *Applied Surface Science* 258 (2012) 6876–6883.
- [44] D. Hegemann, E. Lorusso, M.-I. Butron-Garcia, N.E. Blanchard, P. Rupper, P. Favia, M. Heuberger, M. Vandenbossche, Suppression of Hydrophobic Recovery by Plasma Polymer Films with Vertical Chemical Gradients, *Langmuir* 32 (2016) 651–654.
- [45] E. Bormashenko, G. Chaniel, R. Grynyov, Towards understanding hydrophobic recovery of plasma treated polymers: Storing in high polarity liquids suppresses hydrophobic recovery, *Applied Surface Science* 273 (2013) 549–553.
- [46] A. Vesel, I. Junkar, U. Cvelbar, J. Kovac, M. Mozetic, Surface modification of polyester by oxygen and nitrogen plasma treatment, *Surface and Interface Analysis* 40 (2008) 1444–1453.
- [47] Y. Kusano, Atmospheric Pressure Plasma Processing for Polymer Adhesion: A Review, *The Journal of Adhesion* 90 (2014) 755–777.
- [48] E. Bormashenko, G. Whyman, V. Multanen, E. Shulzinger, G. Chaniel, Physical mechanisms of interaction of cold plasma with polymer surfaces, *Journal of Colloid and Interface Science* 448 (2015) 175–179.
- [49] P. Rupper, M. Amberg, D. Hegemann, M. Heuberger, Optimization of mica surface hydroxylation in water vapor plasma monitored by optical emission spectroscopy, *Applied Surface Science* 509 (2020), 145362.
- [50] M.L. Steen, C.I. Butoi, E.R. Fisher, Identification of Gas-Phase Reactive Species and Chemical Mechanisms Occurring at Plasma–Polymer Surface Interfaces, *Langmuir* 17 (2001) 8156–8166.
- [51] F. Khelifa, S. Ershov, Y. Habibi, R. Snyders, P. Dubois, Free-Radical-Induced Grafting from Plasma Polymer Surfaces, *Chemical Reviews* 116 (2016) 3975–4005.
- [52] L.A. Can-Herrera, A. Ávila-Ortega, S. de la Rosa-García, A.I. Oliva, J.V. Cauch-Rodríguez, J.M. Cervantes-Uc, Surface modification of electrospun polycaprolactone microfibers by air plasma treatment: Effect of plasma power and treatment time, *European Polymer Journal* 84 (2016) 502–513.
- [53] D.O.H. Teare, W. Schofield, R.P. Garrod, J.P. Badyal, Rapid Polymer Brush Growth by TEMPO-Mediated Controlled Free-Radical Polymerization from Swollen Plasma Deposited Poly(maleic anhydride) Initiator Surfaces, *Langmuir: the ACS journal of surfaces and colloids* 21 (2005) 10818–10824.
- [54] S.B. Kedare, R.P. Singh, Genesis and development of DPPH method of antioxidant assay, *J Food Science and Technology* 48 (2011) 412–422.
- [55] R. Teng, H.K. Yasuda, Polymers, Ex Situ Chemical Determination of Free Radicals and Peroxides on Plasma Treated Surfaces, *Plasmas and Polymers* 7 (2002) 57–69.